Ultrafast Angular Momentum Orientation by Linearly Polarized Laser Fields

Kenta Kitano, Hirokazu Hasegawa, and Yasuhiro Ohshima*

Institute for Molecular Science, National Institutes of Natural Sciences, Myodaiji, Okazaki 444-8585, Japan
SOKENDAI (The Graduate University for Advanced Studies), Okazaki 444-8585, Japan

(Received 30 July 2009; published 24 November 2009)

We theoretically show and experimentally verify that a pair of linearly polarized intense femtosecond pulses can create molecular ensembles with oriented rotational angular momentum on an ultrafast (~ps) time scale, when the delay and the mutual polarization between them are appropriately arranged. An asymmetric distribution for $+M$ and $-M$ sublevels relies on quantum interference between rotational wave packets created in stimulated Raman excitation by the first and second pulses. The present approach provides spatiotemporally propagating ensembles, of which the classical perspective is molecules rotating in a clockwise or counterclockwise direction.

DOI: 10.1103/PhysRevLett.103.223002 PACS numbers: 33.20.Sn, 42.50.Hz

When an anisotropic distribution of angular momenta or internuclear axes is introduced in molecular systems, much more information on the internal properties as well as mutual interactions can be extracted than under ordinary gaseous conditions, where isotropic parameters only remain to be assessed after ensemble averaging over angular degrees of freedom [1]. Motivated by the significance of this, various approaches have been proposed and demonstrated to achieve anisotropic distributions. They include focusing and filtering by inhomogeneous external fields [2,3], orientation by a strong electrostatic field [4], optical pumping [5] and dynamical Stark effects [6] by polarized laser excitations, and directional collisions [7], particularly in supersonic expansions [8]. In addition, a recent rapid advance in laser technologies has been leading to extensive adiabatic and nonadiabatic controls of molecular-axis distributions by intense nonresonant laser fields [9], with which the field-matter interaction is beyond the perturbative regime.

In a quantum-mechanical description, the anisotropy of molecular systems is represented as a nonuniform distribution of projections, M, of angular momenta onto a space-fixed (Z) axis. In particular, the system is designated as being oriented when the populations for $+M$ and $-M$ are different, while it is aligned when the populations for $\pm M$ are the same, but those for different $|M|$ differ from one another [1]. In a classical vector model, the signed value of M corresponds to the rotational velocity around the Z axis, so an oriented system is regarded as rotating in the clockwise or counterclockwise direction. In previous studies [5,10], circularly polarized radiations had been exclusively considered as being the way to induce the helical interaction that breaks the right- or left-handed symmetry around the Z axis, which is required for the optical realization of orientation. It is noted that the molecular-axis orientation has already been reported in several studies with intense nonresonant radiation [11–14], but all of them implemented linearly polarized light, and thus were related to the angular-momentum alignment.

In this Letter, we demonstrate the angular-momentum orientation (AMO) in an ultrafast time regime by employing linearly polarized laser fields. Here widely adopted nonadiabatic excitation by nonresonant intense femtosecond (fs) laser fields is implemented. We have found that excitation with a pair of fs pulses induces AMO when the mutual polarization direction and the time delay between them are properly arranged so as to realize a helical field-matter interaction. This phenomenon totally relies on the quantum interference between the rotational wave packets created by the two excitation pulses, which has not been considered so far. The present approach provides orientated molecular systems exhibiting time evolution in a coherent manner, which will be exploited in broader chemical and physical applications.

We first consider the interaction with a linearly polarized nonresonant laser field. A closed-shell symmetric top (benzene in this case) is taken as a molecule sample. Its rotational eigenstate in a field-free condition is denoted as $|J, K, M\rangle$, with the corresponding eigenenergy of $E_{J,K} = hBJ(J+1) + h(C-B)K^2 \equiv \hbar\omega_{J,K}$, where B and C are rotational constants (in Hz unit). Here, the beam propagating direction is set to the Z axis and the angle between the X axis and the polarization vector is denoted as β. Then, the interaction after optical-cycle averaging is represented as

$$\hat{V}(\beta, t) = -\frac{1}{4}[E(t)]^2\Big[\alpha_\perp + \frac{\Delta\alpha}{3}(1 - D^2_{00}) + \frac{\Delta\alpha}{\sqrt{6}}(D^2_{20}e^{2i\beta} + D^2_{-20}e^{-2i\beta})\Big], \tag{1}$$

where $E(t)$ is the pulse envelope of the laser electric field, $\Delta\alpha = \alpha_\parallel - \alpha_\perp$, with static polarizabilities parallel and perpendicular to the molecular symmetry axis, $\alpha_\parallel$ and $\alpha_\perp$, respectively, and D^J_{MK} is the rotational matrix. The matrix elements of $\hat{V}(\beta, t)$ with a field-free basis are diagonal in K, and nonvanishing for $\Delta M = 0, \pm 2$. The transition probabilities for $\Delta M = \pm 2$ are the same as to each other, reflecting a mirror symmetry with respect to the plane in which the Z axis and the polarization vector lie.

To break the right- or left-handed symmetry, an additional interaction should be invoked. To do so, we introduce another linearly polarized pulse with a delay (of τ), of which the polarization is tilted by the angle β, as shown in Fig. 1. Here the polarization of the first pulse is set along the X axis. Then, the transition amplitude from $|J, K, M\rangle$ to $|J', K, M \pm 2\rangle$ in the first order approximation is shown to be proportional to the sum of the two phase factors as follows: if the envelopes of the laser fields are the same for the two pulses,

$$c_{J',K,M\pm 2} \propto e^{-i\Delta\omega_{J',J}\tau} + e^{\mp 2i\beta}, \tag{2}$$

where $\Delta\omega_{J',J} = \omega_{J',K} - \omega_{J,K}$.

Equation (2) indicates that the populations for $M \pm 2$ may be different as a result of interference between the different phase factors for the two pulses. It is noted that β should be $\neq 0, \pi/2$; otherwise, no AMO is created because of the mirror symmetry for the parallel or perpendicular polarization arrangement. It is shown from Eq. (2) that complete constructive and distractive interferences are realized for $\Delta M = +2$ and -2, respectively, in the cases that $\beta = \pi/4$ and $\Delta\omega_{J',J}\tau = \pi/2 + 2\pi n$ or $\beta = -\pi/4$ and $\Delta\omega_{J',J}\tau = 3\pi/2 + 2\pi n$, with n being an integer. For complete constructive and distractive interferences for $\Delta M = -2$ and $+2$, respectively, $\beta = \pi/4$ and $-\pi/4$ are interchanged under the conditions given above, designating the exchange of relative polarizations for the two pulses.

It is noted that $\Delta M = \pm 2$ off diagonal terms in Eq. (1) become smaller when the ellipticity of the laser polarization is increased, and totally vanish for circular polarization. This fact verifies that AMO (along the laser propagation direction) is realized most efficiently when employing a pair of linearly polarized pulses, in the case we adopt the nonadiabatic interaction with nonresonant optical fields.

To check the high-field behavior of the rotational wave packet created by the pair of excitation pulses with skewed mutual polarization, we numerically solved the time-dependent Schrödinger equation (TDSE). The molecular parameters adopted herein are those used in Ref. [15]. In Fig. 2, the final populations starting from $|0, 0, 0\rangle$ are plotted against τ, for $\beta = -\pi/4$. When the laser-field intensity is relatively low (0.1 TW/cm^2), the populations for $|2, 0, \pm 2\rangle$ show completely antiphase sinusoidal modulations to each other, exhibiting maximum or minimum ($=0$) at the expected delay times, $\tau = \pi/(2\Delta\omega_{2,0}) = 1/(24B) \approx 7.3$ ps or $3\pi/(2\Delta\omega_{2,0}) = 1/(8B) \approx 21.9$ ps. For a much higher intensity (1.2 TW/cm^2), they come to show substantial deviations from the dependence represented in Eq. (2), because of coupling with other rotational states, which promotes population transfer to the higher levels via stepwise excitation. Still, large population differences between the $|2, 0, \pm 2\rangle$ states can be realized in the vicinity of the conditions mentioned above.

We next describe an experiment to demonstrate the feasibility of the double-pulse excitation with mutually tilted polarizations. We used an experimental setup constructed for state-selective probing of nonadiabatic excitation of molecular rotation with nonresonant intense fs laser pulses [15,16]. Briefly, the fundamental output from a fs Ti:sapphire laser was fed into a Michelson interferometer, and divided into double pulses of identical energies with a variable delay. A $\lambda/4$ plate was inserted in one arm of the interferometer, and after passing through the plate twice (back and forth) the polarization direction of one pulse was rotated by 45° with respect to the other pulse. These pump pulses were merged and then collinearly focused onto jet-cooled benzene ensembles in a molecular beam. The rota-

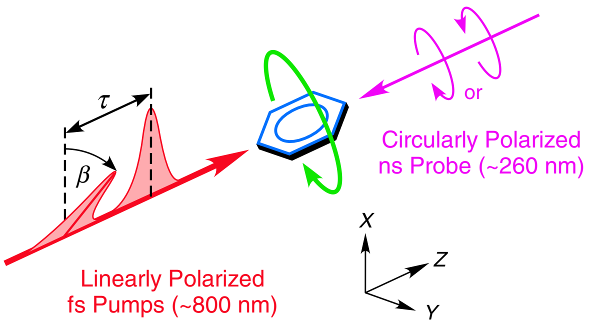

FIG. 1 (color online). Experimental scheme to create and observe the angular-momentum orientation in molecular rotation.

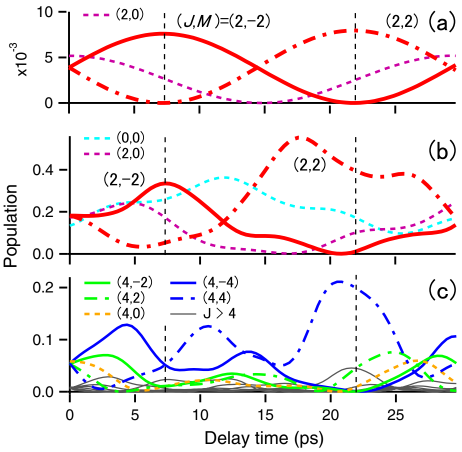

FIG. 2 (color online). Calculated populations in a rotational wave packet created by double-pulse excitation of the $|0, 0, 0\rangle$ initial state, plotted against the delay, τ, between the two pulses. β is set to $-\pi/4$. A Gaussian time profile with duration of 200 fs (FWHM) is used for the calculation. The laser peak intensity for each pulse is (a) 0.1 TW/cm^2, and (b),(c) 1.2 TW/cm^2. In panel (a), the vertical scale is expanded so that the population of $|0, 0, 0\rangle$ is out of the range. For 1.2 TW/cm^2, populations of $J = 0$ and 2 are shown in panel (b) while those of $J \geq 4$ in (c) for clarity.

tional temperature was adiabatically cooled down to 0.9 K, so that the initial state distribution was predominantly populated by the five lowest levels, $J_{|K|} = 0_0$, 1_0, 1_1, 2_2, and 3_3, in the different nuclear-spin manifolds [15]. A linear chirp was applied to stretch the pulse duration to 200 fs so as to avoid unwanted tunneling ionization by the fs pulses. After the excitation by the fs pump pulses, the excitation spectrum of the benzene molecule was recorded by (1 + 1) resonance enhanced multiphoton ionization (REMPI) via the $S_1 - S_0$ 6_0^1 transition. The probe pulse with a 0.06 cm^{-1} bandwidth was delivered as a doubled output from a nanosecond dye laser. The probe pulse was circularly polarized after passing through another $\lambda/4$ plate.

Figure 3 shows a typical example of the REMPI excitation spectra, recorded after excitation by a fs pulse pair, of which the mutual polarization angle was set at $\pi/4$ or $-\pi/4$. The delay time (7.3 ps) is optimum in the low-field limit to achieve the largest orientation in the $J_{|K|} = 2_0$ and 3_2 states, i.e., $\tau = \pi/(2\Delta\omega_{2,0}) = \pi/(2\Delta\omega_{3,2}) = 1/(24B)$, as discussed before. Since the delay time also provides substantial population differences between $\pm M$ sublevels in many other rotational states, e.g., 2_1, 2_2, 3_1, and 4_3, P-branch transitions from these states showed pronounced intensity changes against the circularity of the probe pulse. This experimental finding verifies a successful realization of AMO in the vibronic ground state of benzene. The relative intensities for the right- and left-handed probe conditions were entirely reversed when the polarization angle was changed form $\pi/4$ to $-\pi/4$. This is a natural consequence of the symmetry concerning the right- to left-handed reversal of the rotational angular momentum and the helicity of the probe photon. At this delay time, all of the probed rotational states showed the same preference in orientation so that all of the observed transitions for $\beta = \pi/4$ ($-\pi/4$) appeared stronger (weaker) for the right-handed probe than those for the opposite circularity.

The field intensity was evaluated as 1.2 $\mathrm{TW/cm}^2$ from a comparison of the observed and simulated spectra for single-pulse excitation by either of the fs pulse pair. The derived value reasonably agrees with that estimated from the experimentally determined pulse energy, duration, and beam diameter. By adopting the intensity, spectra for the skewed double-pulse excitation are simulated by a TDSE calculation while considering the initial distribution at 0.9 K, as shown in the top panel of Fig. 3. The matchup to the observed ones is satisfactory.

The degree of orientation, $\langle \hat{J}_Z \rangle \equiv \langle J_Z \rangle / \sqrt{\langle J^2 \rangle}$, was evaluated by the TDSE calculation for the ensemble starting from the five lowest rotational levels (with 19 M sublevels in total) and their nuclear-spin weighted average, as shown in Fig. 4. The orientation shows an oscillatory change against the delay between the pulse pair. The largest value of $|\langle \hat{J}_Z \rangle|$ reaches to 0.6 for $J_K = 0_0$. The oscillation amplitude of $\langle \hat{J}_Z \rangle$ gradually decreases for the initial states with larger J, due to a partial cancellation by contributions from different M sublevels. Nevertheless, the gross average of the five states keeps the largest $|\langle \hat{J}_Z \rangle|$ of ~0.2. $\langle \hat{J}_Z \rangle$ for an ensemble of different J_K levels shows revival transients, exhibiting dispersionlike shapes with ~10 ps duration at around the multiples of the half revival time, $T_{\mathrm{rev}}/2 = 1/(4B)$, which look similar to those appearing in molecular-axis alignment and orientation [9,11,12,14]. In

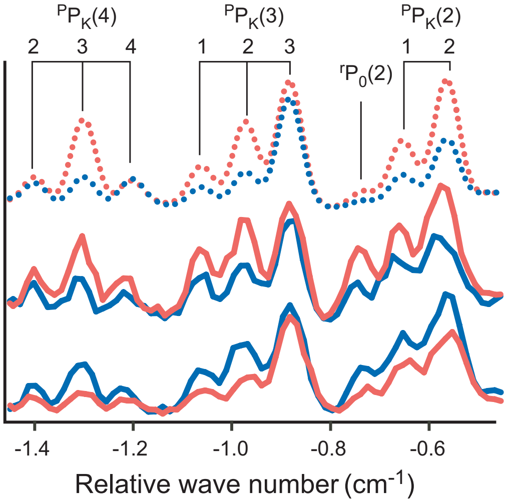

FIG. 3 (color online). Excitation spectra of the P-branch region in the $S_1 - S_0$ 6_0^1 band of benzene after fs double-pulse excitation with τ set to 7.3 ps, recorded with the right-handed [dark gray (blue) lines] and left-handed [light gray (red) lines] polarized probe pulse. The middle and lower panels show experimentally observed ones for $\beta = -\pi/4$ and $\pi/4$, respectively, while the upper one is simulated for $\beta = -\pi/4$ with a laser peak intensity of 1.2 $\mathrm{TW/cm}^2$ for each pulse.

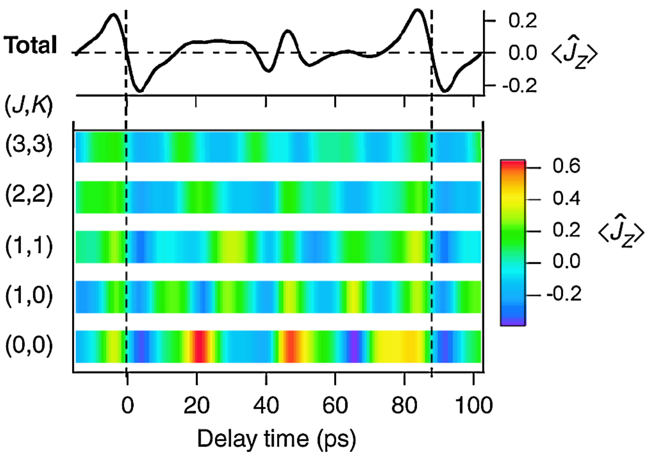

FIG. 4 (color online). Delay-time dependence of the degree of orientation, $\langle \hat{J}_Z \rangle$, for wave packets created from the five lowest rotational levels, as well as their nuclear-spin weighted average. β is set to $-\pi/4$ and the laser peak intensity is 1.2 $\mathrm{TW/cm}^2$ for each pulse. Vertical broken lines indicate delay time at zero and $T_{\mathrm{rev}} \approx 87.9$ ps.

particular, $\langle \hat{J}_Z \rangle$ in the vicinity of the zero delay rapidly reaches its maximum (or minimum) within $\approx +4$ (or -4 ps), which is much shorter than the time scale of rotation, $T_{\rm rev}$.

The present approach to attaining AMO has multifold significances. First, the AMO achieved here is solely due to interferences between the wave packets created by linearly polarized light fields. This is totally different from approaches so far adopted, in which an unbalanced population for $\pm M$ sublevels is a direct consequence of optical transitions by circularly polarized light with $\Delta M = +2$ or -2, exclusively [10]. In other words, the previous scheme is well within the classical perspective, where the transition dipole follows the right- or left-handed rotating optical field when the rotational period matches with the characteristic time for molecular rotation. On the other hand, the present approach is based on a purely quantum effect, as demonstrated by the fact that two excitation pulses can be temporally separated with no overlap, and the relative optical phase between them has no affect on the results.

Second, oriented states provided in the present AMO are wave packets or their ensembles with respect to the initially populated eigenstates, and thus exhibit spatiotemporal propagation in an ultrafast time regime (~ps), which is a quantum-mechanical representation of clockwise or counterclockwise rotation of molecules. Such a nonstationary microscopic state of unidirectionally circulating motion has rarely been realized, whereas a time-dependent molecular alignment has been extensively studied so far [9]. The single previous study relevant to AMO by short pulse radiation was on the optical centrifuge [17]. In the resultant state of motion, the distributions for J_Z as well as J are confined to a very limited range, since the optical field duration was longer than the characteristic time for rotation, and thus the acceleration of rotation had been achieved in an adiabatic regime [18]. This is in sharp contrast to the present case, where the excitation pulse is much shorter than the rotational period, and the state thus nonadiabatically created is the coherent superposition of widely spread J levels.

Third, the present scheme is versatile to attain the AMO in the electronic ground state of any molecular system with an anisotropic polarizability, and it is not necessary to tune the excitation wavelength to the transitions of the system. This method need not be limited to control over the rotational motion. The circular direction of molecular vibrations, e.g., the internal rotation or torsion, can also be controlled by the present scheme, especially when the molecular-axis alignment is coupled to the nonadiabatic vibrational excitation, as demonstrated in a recent study [19]. It may also be possible to orient the electronic angular momentum in 2D or 3D isotropic atomic or molecular systems, when their relevant energy intervals are small enough to be covered by the laser bandwidth, e.g., fine-structure splitting or M-sublevel splitting induced by an external field. Such an AMO is useful for ultrafast control of the magnetic and optical responses of the ensemble under consideration. Directional control of the angular momentum will possibly be extended even in the condensed phase, when the relaxation that causes a loss of coherence in the created wave packets is slower than the orientation attainment well within the wave packet oscillation, as shown in Fig. 4.

This work was partly supported by Grants-in-Aid from MEXT Japan (18244120 and 18750020), and the RIKEN-IMS joint program on "Extreme Photonics." Additional financial support from the Mitsubishi Foundation is also appreciated.

---

*ohshima@ims.ac.jp

[1] K. Blum, *Density Matrix Theory and Applications* (Plenum, New York, 1996), Chap. 7.
[2] D. H. Parker and R. B. Bernstein, Annu. Rev. Phys. Chem. **40**, 561 (1989).
[3] A. Gijsbertsen *et al.*, Phys. Rev. Lett. **99**, 213003 (2007).
[4] D. T. Moore, L. Oudejans, and R. E. Miller, J. Chem. Phys. **110**, 197 (1999).
[5] W. Happer, Rev. Mod. Phys. **44**, 169 (1972).
[6] J. Qi *et al.*, Phys. Rev. Lett. **83**, 288 (1999).
[7] K. T. Lorenz *et al.*, Science **293**, 2063 (2001).
[8] F. Pirani *et al.*, J. Chem. Phys. **119**, 265 (2003).
[9] H. Stapelfeldt and T. Seideman, Rev. Mod. Phys. **75**, 543 (2003).
[10] N. C.-M. Bartlett *et al.*, J. Chem. Phys. **129**, 084312 (2008).
[11] H. Sakai, S. Minemoto, H. Nanjo, H. Tanji, and T. Suzuki, Phys. Rev. Lett. **90**, 083001 (2003).
[12] A. Goban, S. Minemoto, and H. Sakai, Phys. Rev. Lett. **101**, 013001 (2008).
[13] L. Holmegaard *et al.*, Phys. Rev. Lett. **102**, 023001 (2009).
[14] O. Ghafur *et al.*, Nature Phys. **5**, 289 (2009).
[15] H. Hasegawa and Y. Ohshima, Chem. Phys. Lett. **454**, 148 (2008).
[16] H. Hasegawa and Y. Ohshima, Phys. Rev. Lett. **101**, 053002 (2008).
[17] D. M. Villeneuve *et al.*, Phys. Rev. Lett. **85**, 542 (2000).
[18] M. Spanner and M. Yu. Ivanov, J. Chem. Phys. **114**, 3456 (2001).
[19] C. B. Madsen *et al.*, Phys. Rev. Lett. **102**, 073007 (2009).